J Membrane Biol (2014) 247:1031–1041
DOI 10.1007/s00232-014-9712-6

Amphipols and Photosynthetic Light-Harvesting Pigment-Protein Complexes

Milena Opačić · Grégory Durand · Michael Bosco · Ange Polidori · Jean-Luc Popot

Received: 10 May 2014 / Accepted: 23 July 2014 / Published online: 9 August 2014

Abstract The trimeric light-harvesting complexes II (LHCII) of plants and green algae are pigment-protein complexes involved in light harvesting and photoprotection. Different conformational states have been proposed to be responsible for their different functions. At present, detergent-solubilized LHCII is used as a model for the "light-harvesting conformation", whereas the "quenched conformation" is mimicked by LHCII aggregates. However, none of these conditions seem to perfectly reproduce the properties of LHCII in vivo. In addition, several monomeric LHC complexes are not fully stable in detergent. There is thus a need to find conditions that allow analyzing LHCs in vitro in stable and, hopefully, more native-like conformations. Here, we report a study of LHCII, the major antenna complex of plants, in complex with amphipols. We have trapped trimeric LHCII and monomeric Lhcb1 with either polyanionic or non-ionic amphipols and studied the effect of these polymers on the properties of the complexes. We show that, as compared to detergent solutions, amphipols have a stabilizing effect on LHCII. We also show that the average fluorescence lifetime of LHCII trapped in an anionic amphipol is ~30 % shorter than in α-dodecylmaltoside, due to the presence of a conformation with 230-ps lifetime that is not present in detergent solutions.

Keywords Neoxanthin · Fluorescence · Light-harvesting complexes · Membrane protein · A8-35 · Non-ionic amphipols

Abbreviations

A8-35	A specific type of polyacrylate-based amphipol
AIBN	Azobisisobutyronitrile
APol	Amphipol
BR	Bacteriorhodopsin
Car	Carotenoid
CD	Circular dichroism
Chl	Chlorophyll
LHCII	LHCII trimers
α-DDM	*N*-dodecyl-α-D-maltoside
β-DDM	*N*-dodecyl-β-D-maltoside
MD	Molecular dynamics
MP	Membrane protein
NA13	A specific batch of non-ionic APol
NAPol	Non-ionic APol
NPQ	Non-photochemical quenching
SEC	Size exclusion chromatography
TR	Thiol-based transfer agent

Electronic supplementary material The online version of this article (doi:10.1007/s00232-014-9712-6) contains supplementary material, which is available to authorized users.

M. Opačić (✉)
Department of Physics and Astronomy, Faculty of Sciences, VU University Amsterdam, De Boelelaan 1081, 1081 HV Amsterdam, The Netherlands
e-mail: milenaopacic@gmail.com

G. Durand · M. Bosco · A. Polidori
Equipe Chimie Bioorganique et Systèmes Amphiphiles, Université d'Avignon, 33 rue Louis Pasteur, 84000 Avignon, France

G. Durand · M. Bosco · A. Polidori
Institut des Biomolécules Max Mousseron (UMR 5247), 15 Avenue Charles Flahault, 34093 Montpellier Cedex 05, France

J.-L. Popot
Unité Mixte de Recherche 7099, Centre National de la Recherche Scientifique and Université Paris 7, Institut de Biologie Physico-Chimique (FRC 550), 13 rue Pierre-et-Marie Curie, 75005 Paris, France

Introduction

The light-harvesting complex II (LHCII) of photosynthetic organisms is the most abundant membrane protein (MP) on earth. LHCII is a heterotrimer composed of monomeric antenna proteins Lhcb1, Lhcb2, and Lhcb3, which are associated in different combinations (Caffarri et al. 2004; Jansson 1999). Each monomer ($M \approx 25$ kDa) features three transmembrane α-helices, to which are bound eight chlorophylls *a* (Chl*a*), six chlorophylls *b* (Chl*b*), and four carotenoids (Cars): two luteins, one neoxanthin, and one violaxanthin (Liu et al. 2004). The trimeric LHCII is involved in light harvesting for photosystems I and II (PSI and PSII) (Croce and van Amerongen 2011; Wientjes et al. 2013) and in non-photochemical quenching (NPQ) (Ballottari et al. 2012). NPQ is a mechanism, triggered by low pH in the thylakoid lumen, that plants have developed to protect themselves against photodamage, dissipating the light absorbed in excess as heat (Müller et al. 2001; Ruban et al. 2012). It has been proposed that LHCII plays one of the major roles in NPQ by switching from a light-harvesting conformational state, known as "active" state, to an energy "dissipative" state (Ruban et al. 2007, 2012).

In order to understand the structural basis of the regulatory mechanism, the conformational states of LHCII in different microenvironments have been extensively studied (Barros et al. 2009; Belgio et al. 2012; Moya et al. 2001; Pascal et al. 2005; Ruban et al. 2007), spectroscopic properties like fluorescence quantum yield and fluorescence lifetime being amongst the most widely used parameters to monitor them. LHCII trimers in detergent solution are generally used as a model for the light-harvesting conformation, whereas the "quenched conformation" is mimicked by LHCII aggregates (see e.g. van Oort et al. 2007). The exact lifetime of LHCII in its light-harvesting conformation is a matter of debate, because differences have been observed between the properties of membrane-bound and detergent-solubilized LHCII. The average fluorescence lifetime of the active state of LHCII in thylakoids is ∼2 ns, whereas for the dissipative one it ranges from 0.6 to 0.8 ns (Belgio et al. 2012). In detergent solution, LHCII is highly fluorescent and usually shows an average lifetime of the excited state of ∼3.6 ns (see e.g. Moya et al. 2001). In LHCII crystals, the average fluorescence lifetime is ∼0.89 ns (Pascal et al. 2005). For aggregates of LHCII, it depends on the degree of aggregation; for example, lamellar aggregates of LHCII from spinach exhibit a dominant component of 0.65 ns, with an average lifetime of 0.70 ns (Miloslavina et al. 2008). For LHCII incorporated in liposomes at different lipid/protein ratios, the average fluorescence lifetime ranges from ∼0.9 to 1.7 ns (Moya et al. 2001). In studies carried out with the trimeric LHCII assembled in lipid nanodiscs in a detergent-free environment, the conformation of LHCII was observed to differ from that in detergent solution, but no clear quenching was detected (Pandit et al. 2011).

In the present work, we explore a new approach to studying the conformational states of LHCII trimers (hereafter, LHCII) in a detergent-free environment. Detergents are known to destabilize MPs (see e.g. Refs. Bowie 2001; Garavito and Ferguson-Miller 2001; Popot 2010; Privé 2007; Rosenbusch 2001). In particular, they can compete with protein–protein and protein–lipid interactions (see e.g. Breyton et al. 1997; Levi et al. 2000; Lund et al. 1989). Amphipols (APols) are short amphipathic polymers designed to keep MPs soluble in aqueous solution in the absence of detergent (Popot et al. 2011; Tribet et al. 1996; Zoonens and Popot 2014). APols adsorb onto the transmembrane hydrophobic surface of MPs, forming a compact, ∼2-nm-thick layer (Althoff et al. 2011; Gohon et al. 2008; Liao et al. 2014). Due to their high affinity and low critical association concentration (Giusti et al. 2012), APols remain bound to MPs even at very high dilutions (Tribet et al. 2009; Zoonens et al. 2007). Nevertheless, they are exchangeable for detergents, lipids, and other APols (Nagy et al. 2001; Polovinkin et al. 2014; Tribet et al. 1997, 2009; Zoonens et al. 2007). As transfer from detergent solution to APols improves the stability of most MPs (reviewed in Refs. Kleinschmidt and Popot 2014; Popot 2010; Popot et al. 2011; Zoonens and Popot 2014), it is of interest to investigate the effect of APols on LHC complexes, several of which have been found to be unstable in detergent solution (e.g. Mozzo et al. 2006; Morosinotto et al. 2005).

The best-characterized APol, called A8-35 (Fig. 1a), was introduced in the mid-1990s (Tribet et al. 1996) and has been extensively used since (reviewed by Popot et al. 2011; Zoonens and Popot 2014). A8-35 is comprised of a mixture of short amphipathic polymers with a polyacrylate backbone onto which two kinds of side chains have been randomly grafted: ∼25 % of its units carry an octylamide side chain, ∼40 % an isopropylamide one, and ∼35 % an underivatized carboxylate (Tribet et al. 1996), with an average molecular mass of ∼4.3 kDa (Giusti et al. 2014). In aqueous solutions, A8-35 assembles into small globular particles containing an average of ∼9 molecules, with a total mass of ∼40 kDa (Gohon et al. 2006). Because its solubility is due to the negative charges carried by the carboxylate groups, A8-35 cannot be used for studies carried out at low pH (Gohon et al. 2006) nor in the presence of multivalent cations (Picard et al. 2006). This limitation has led to the development of pH-insensitive APols, such as phosphorylcholine-based APols (Diab et al. 2007), sulfonated APols (Dahmane et al. 2011), and non-ionic APols

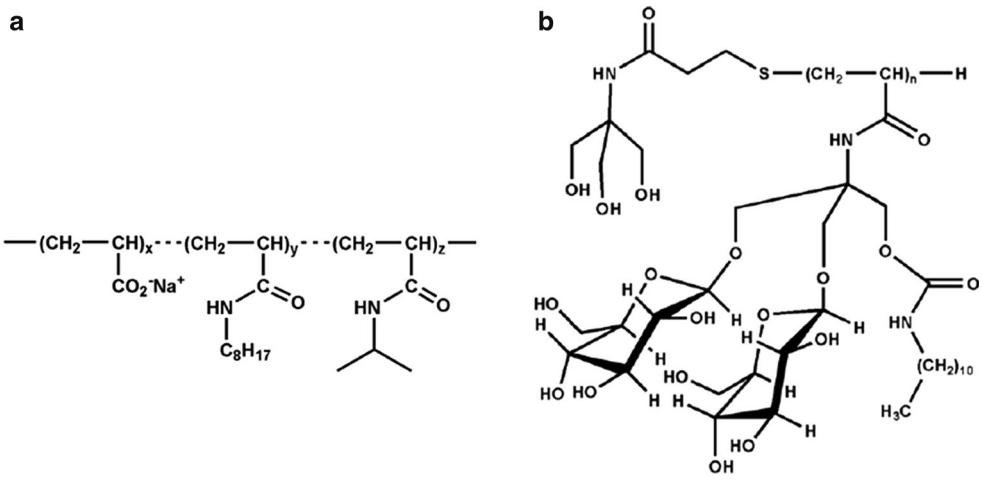

Fig. 1 Chemical structures of the two types of amphipols used in the present work. **a** A8-35, a polyacrylate-based APol (from Tribet et al. 1996); $x \approx 35$ %, $y \approx 25$ %, $z \approx 40$ %. **b** NA13, a non-ionic, homopolymeric, glucose-based APol (from Sharma et al. 2012); $n \approx 19$

(NAPols) (Sharma et al. 2012), the solubility of the latter being due to the presence of glucose moieties (Fig. 1b). Comparative experiments suggest that NAPols may stabilize MPs even better than A8-35 (Bazzacco et al. 2012).

With the aim of exploring novel possibilities for studying photosynthetic antenna proteins out of the membrane, we have examined the effect of A8-35 and NAPols on the solubility, dispersity, stability, and functionality of higher plant trimeric and monomeric LHCII complexes.

Materials and Methods

Arabidopsis thaliana plants were grown in a growing chamber at a day/night regime of 14/10 h with light intensity of 100 µmol photons·m^{-2}·s^{-1}, an average temperature of 20 °C, and 70 % relative humidity. Plants were usually harvested after a growth period of 7–8 weeks. Amphipol A8-35 and *n*–dodecyl-α-D-maltoside (α-DDM) were purchased from Anatrace, polystyrene Bio-Beads SM-2 (Bio-Beads) from Bio-Rad, and pinacyanol chloride from Sigma.

Isolation and Solubilization of Thylakoid Membranes from *Arabidopsis thaliana* and Purification of the LHCII Trimers

Thylakoid membranes were purified according to published procedures (Bassi and Simpson 1987; Croce et al. 1996). Their solubilization was performed essentially as described (Wientjes et al. 2009). In short, thylakoids were thawed on ice in the dark. They were diluted using 10 mM HEPES, pH 7.6, and centrifuged at 12,000 × *g* for 15 min at 4 °C in a Sigma 1–15 k centrifuge. The pellet was carefully resuspended in 10 mM HEPES, pH 7.6, 5 mM EDTA, and centrifuged at 12,000 × *g* for 12 min at 4 °C. After removal of the supernatant, the pellet was treated the same

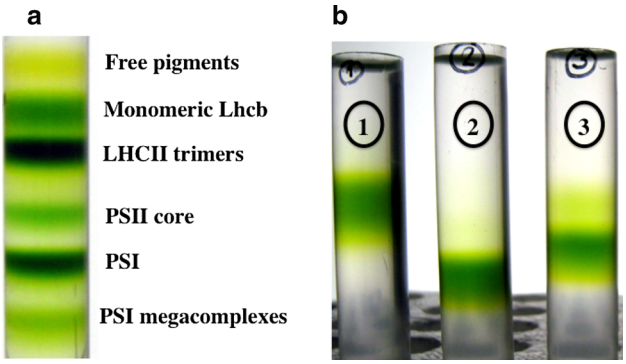

Fig. 2 **a** Sucrose gradient fractionation of thylakoids from *Arabidopsis thaliana* solubilized using 0.6 % α-DDM. **b** Sucrose gradient analysis of purified LHCII complexes in various surfactants: ① A8-35-trapped; ② NA13-trapped; ③ in 0.03 % α-DDM. Gradients ① and ② contained no surfactant, gradient ③ 0.03 % α-DDM

way as above, but using only 10 mM HEPES buffer, pH 7.6, to wash away residual EDTA. The final pellet was resuspended in 500 µL of 10 mM HEPES, pH 7.6, and 500 µL of the solubilization buffer (same + 1.2 % α-DDM) were added. The mixture was vortexed for 1 min before being centrifuged at 12,000 × *g* for 12 min at 4 °C. The supernatant was loaded onto sucrose gradients (15 mM HEPES, pH 7.6, 0.1–1 M sucrose, 0.03 % α-DDM) and ultracentrifuged for 16 h at 280,000 × *g* at 4 °C in a SW41Ti Beckman rotor. Band 3, corresponding to LHCII trimers (Fig. 2a), was collected with a syringe and either studied immediately or aliquoted, frozen in liquid nitrogen, and stored at −80 °C.

Overexpression of Lhcb1 and Reconstitution of the Recombinant Protein

Overexpression and reconstitution of Lhcb1 were carried out as described (Caffarri et al. 2007). For 100 µg of apoprotein, 70 µg of chlorophyll (2.9:1 molar ratio of

Chl*a*/Chl*b*) and 11 μg of total carotenoid extract (Natali et al. 2014) were used.

Protein and Pigment Concentration Determination

The pigment complement of the complexes was analysed by fitting the acetone extract spectrum with the spectra of the individual pigments (Croce et al. 2002) and by HPLC analysis (Gilmore and Yamamoto 1991).

Synthesis of Non-Ionic Amphipol NA13

The synthesis of NA13 was carried out as described (Sharma et al. 2012; see Scheme 1 in S.I.). In brief, the synthesis is based on the free radical homopolymerization of an acetylated diglucosylated amphiphilic monomer (M) (Sharma et al. 2011). Polymerization is performed in refluxing tetrahydrofuran in the presence of a benzoylated thiol-based transfer agent (TR), with azobisisobutyronitrile (AIBN) (0.5 equiv/TR) as an initiator. The number-average degree of polymerization is determined by the initial molar ratio of M to TR (20:1). The reaction was monitored by thin-layer chromatography and carried out until complete disappearance of the monomer. The acetylated polymer was purified by preparative size exclusion chromatography (SEC) on hydroxylpropylated cross-linked dextran in a 1:1 CH_3OH/CH_2Cl_2 mixture. Thanks to the aromatic groups grafted onto TR, the number-average degree of polymerization of the batch used in the present work, NA13, was determined by UV and ^{1}H NMR measurements to be $\sim$20. Simultaneous deprotection of the acetyl and benzoyl groups was achieved under the Zemplén conditions, yielding NA13, with an average molecular mass of $\sim$13 kDa.

Trapping of LHCII Trimers and Recombinant Monomers of Lhcb1 with Amphipols

LHCII and recombinant Lhcb1 monomers in 0.03 % α-DDM were mixed with either A8-35 or NA13 in a 1:5 protein/APol mass ratio and the samples incubated for 45 min on ice in the dark, after which Bio-Beads were added at a 10:1 Bio-Bead/detergent mass ratio. One aliquot of LHCII received neither APol nor Bio-Beads ("reference sample" in detergent), whereas another was supplemented with Bio-Beads in the absence of APols ("negative control" sample). The samples were incubated overnight at 4 °C in the dark with constant stirring, after which the Bio-Beads were removed by centrifugation. To check on the integrity of the proteins, the supernatants were loaded onto sucrose gradients (15 mM HEPES, pH 7.6, 0.1–1 M sucrose). The gradients used for purifying APol-trapped LHCII and Lhcb1 and for the negative control contained no surfactant (i.e. neither APol nor detergent), whereas those used for the reference samples contained 0.03 % α-DDM. After ultracentrifugation for 18 h at 280,000 × *g* at 4 °C in a SW41Ti Beckman rotor, the green bands were collected with a syringe and immediately used for further analysis.

A8-35-Trapped LHCII Trimers in Different Ionic Strength Conditions

A sample of LHCII trimers was trapped with A8-35 as described above and divided into six aliquots. One aliquot was kept as such, whereas the others were adjusted to final concentrations of 25, 75, 125, 200, or 500 mM NaCl. The samples were then centrifuged as described above in sucrose gradients containing the same NaCl concentration as the sample and no surfactant. Bands were collected with a syringe and used for analysis. The same procedure was used for LHCII trimers in α-DDM solutions, with the sole difference that the gradients contained 0.03 % α-DDM.

LHCII Trimers at Various pH

Three samples of LHCII trimers in 15 mM HEPES buffer supplemented with 0.03 % α-DDM were diluted 3× with either 15 mM MES buffer, pH 5.5, or 15 mM HEPES buffer, pH 6.5, or 15 mM HEPES buffer, pH 7.6, containing 0.03 % α-DDM. After a short incubation in the dark on ice, each sample was divided into two aliquots, one of which was supplemented with NA13 and the other kept in α-DDM buffer. After half of an hour on ice, Bio-Beads were added to the samples supplemented with NA13 and all samples incubated overnight at 4 °C in the dark with constant stirring. After removal of the Bio-Beads by centrifugation, the supernatants were loaded onto sucrose gradients prepared with the same buffer as the sample. Absorption and CD measurements were carried out on fractions collected from the gradients.

Steady-State Spectroscopy

Absorption spectra were recorded on a Varian Cary 4000 UV–Visible spectrophotometer, fluorescence emission spectra on a Fluorolog 3.22 fluorometer (HORIBA Jobin–Yvon). CD measurements were carried out using a Chirascan-plus CD spectrometer (Applied Photophysics). Absorption and fluorescence spectroscopy measurements were performed at room temperature (RT). CD spectra were recorded at 20 °C, as well as in a 20–90 °C temperature range, in which case the temperature was increased in 5 °C steps at time intervals of 90 s. Samples used for recording fluorescence emission spectra were diluted to obtain an OD of 0.05 cm^{-1} at the Q_Y maximum. Fluorescence emission spectra were recorded using three excitation wavelengths: 440, 475, and 500 nm. The buffer used for diluting the LHCII

trimers and Lhcb1 monomers in detergent micelles was 15 mM HEPES, pH 7.6, 0.03 % α-DDM, that used for diluting A8-35-trapped trimers the same without surfactant, those for diluting NAPol-trapped trimers surfactant-free 15 mM MES, pH 5.5, 15 mM HEPES, pH 6.5, or 15 mM HEPES, pH 7.6. When needed, dilution buffers contained appropriate concentrations of NaCl.

Time-Resolved Fluorescence Spectroscopy

Time-correlation single-photon counting measurements were carried out using a PicoQuant FluoTime 200 time-resolved spectrometer, with an excitation wavelength of 468 nm. Fluorescence emission was monitored at 680 nm. The instrument response function of 88 ps (full width at half maximum) was determined using pinacyanol chloride, whose fluorescence lifetime is 6 ps (van Oort et al. 2008), or a Ludox scattering solution. Samples were diluted to obtain an OD of 0.05 cm^{-1} at the Q_Y maximum. Dilution buffers were the same as described above. Measurements were carried out at 10 °C, with constant stirring. Data were analysed using the TRFA software (version 1.4), SSTC Department of System Analysis, Belarusian State University, Belarus.

Size Exclusion Chromatography

SEC measurements were carried out at room temperature using a Shimadzu 10-A liquid chromatography system with a Superdex 200 10/300 GL column. Injection volumes were 200 µL. The elution buffer was 15 mM HEPES, with or without 0.03 % α-DDM, with NaCl at the same concentration as in the sample. Detection wavelengths were 280, 440, 475, and 675 nm.

Results and Discussion

In search for conditions that increase the stability of LHC-purified complexes and preserve their native properties, we have tested the effect of APols on LHCII trimers and Lhcb1 monomers. Two APols were chosen: a polyanionic APol, A8-35, which is by far the most extensively characterized APol, and a homopolymeric non-ionic APol, NAPol, which can be used in a broader pH range. The batch of NAPol used for the present study had an average molecular mass of ~13 kDa and is referred to as NA13.

Trapping of LHCII Trimers and Lhcb1 Monomers with A8-35 and NA13

LHCII trimers in α-DDM solution, purified from *A. thaliana*, were supplemented with either A8-35 or NA13, and the detergent removed using Bio-Beads, after which ultracentrifugation in sucrose gradients was performed in order to examine the solubility, integrity and dispersity of the complexes. Each gradient was found to contain a single band (Fig. 2b). The faster migration of NA13-trapped versus A8-35-trapped LHCII is most likely due to two factors: (*i*) a probable difference in the mass of bound APol—bacteriorhodopsin (BR) binds, in mass, twice more NAPol than A8-35 (Gohon et al. 2008; Sharma et al. 2012)—and (*ii*) the higher density of NAPols (1.297 g mL^{-1}; Sharma et al. 2012) versus A8-35 (1.155 g mL^{-1}; Gohon et al. 2008).

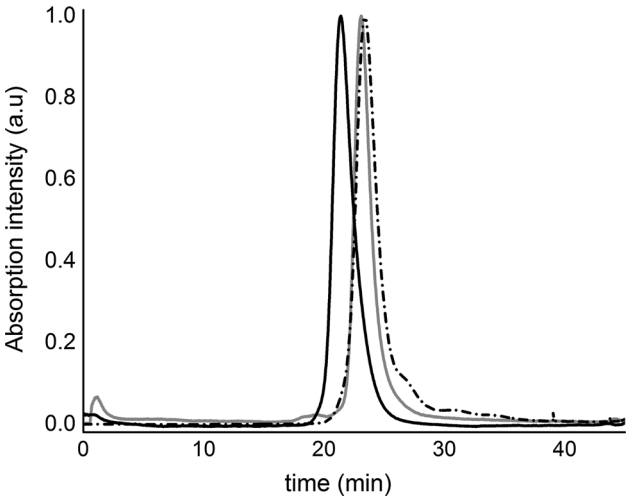

Fig. 3 Size exclusion chromatography analysis of NA13-trapped LHCII (*grey;* detection wavelength 436 nm), A8-35-trapped LHCII (*solid black line*; detection wavelength 437 nm), and α-DDM-solubilized LHCII (*dash-dotted black line*; detection wavelength 439 nm)

Upon SEC analysis, A8-35- and NA13-trapped trimers eluted as a single peak, confirming their homogeneity (Fig. 3). Based on observations with BR/APol complexes (Sharma et al. 2012), the difference in elution volumes between A8-35-trapped and NA13-trapped or DDM-solubilized LHCII most likely reflects different interactions of charged A8-35 versus uncharged NA13 and DDM with the column material more than actual size differences. The Chl *a*/*b* ratio of LHCII in α-DDM, A8-35, and NA13 was ~1.3 and the Chl/Car molar ratio ~3.9, with the xanthophylls neoxanthin, violaxanthin, and lutein being present in each sample in the same ratio, indicating that trapping with APols did not affect pigment binding. The same procedure was applied to trap the reconstituted monomer Lhcb1 with A8-35. Again, a single band was observed in sucrose gradients (*not shown*), and the homogeneity of the preparation was confirmed by SEC fractionation (Fig. S1).

Amphipol-Trapped Trimeric LHCII and Monomeric Lhcb are Properly Folded

Steady-state fluorescence emission spectra of LHCII trimers in the three environments exhibited one clear emission band

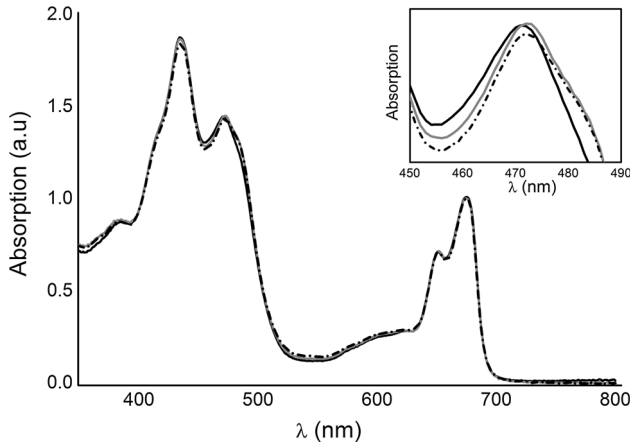

Fig. 4 Absorption spectra at room temperature of LHCII trimers in 0.03 % α-DDM (*black dash-dotted line*) and after trapping with either A8-35 (*solid black line*) or NA13 (*solid grey line*). *Inset* shows enlargement of the Soret region. The spectra were normalized on the region of Q_Y absorption

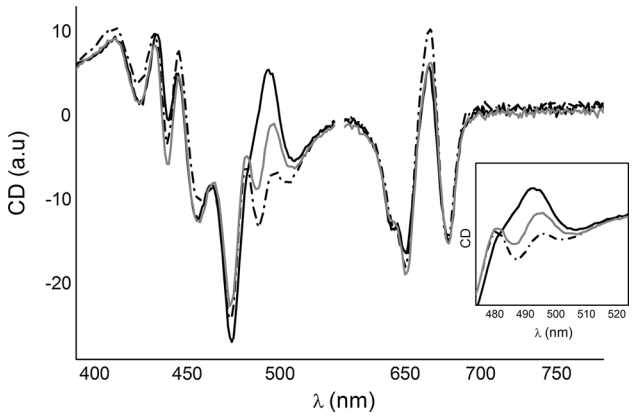

Fig. 5 Circular dichroism spectra at 20 °C of LHCII in 0.03 % α-DDM (*dash-dotted black line*), A8-35-trapped (*solid black line*) and NA13-trapped (*solid grey line*). *Inset* shows enlarged region from 475 to 530 nm. Spectra are normalized to the ellipticity at 675 nm

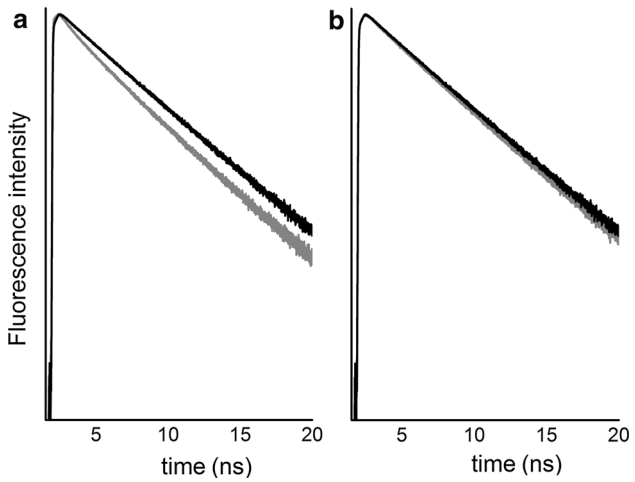

Fig. 6 Fluorescence intensity decays of **a** A8-35-trapped LHCII before (*grey*) and after (*black*) addition of 0.06 % α-DDM and **b** NA13-trapped LHCII before (*grey*), and after (*black*) addition of 0.06 % α-DDM

with maximum at 681 nm (and its corresponding vibronic band centred around 740 nm) independently of the excitation wavelength (Fig. S2). This confirmed the absence of disconnected pigments in the preparations and, therefore, the absence of protein denaturation. Similar results were obtained for A8-35-trapped recombinant Lhcb1, confirming that also the monomeric complex is correctly folded in APols (not shown).

Effect of pH on α-DDM-Solubilized and NA13-Trapped LHCII

Samples of α-DDM-solubilized and NA13-trapped LHCII were studied at pH 5.5, 6.5, and 7.6 (see "Materials and Methods" section). In each case, a single green band was observed following ultracentrifugation on sucrose gradients (Fig. S3). The green bands collected from the gradients had the same absorption and CD spectra in all three pH conditions (data not shown). LHCII therefore remains trimeric and stable at a pH as low as 5.5 whether it is solubilized in α-DDM or trapped with NA13.

Spectroscopic Features of Amphipol-Trapped LHCII

To explore in more detail the effects of the two APols on the structural organization of trimeric LHCII, absorption (Fig. 4), fluorescence (Fig. S3) and CD (Fig. 5), measurements were performed, along with fluorescence lifetime ones (Fig. 6; Table 1).

Absorption spectra of LHCII trapped in either A8-35 or NA13 or solubilized in α-DDM were practically identical in the Q_Y absorption region, but A8-35-trapped trimers exhibited a difference (Fig. 4) in the 480–490 nm spectral region, assigned to neoxanthin (Croce et al. 1999b).

Table 1 Fluorescence lifetimes and amplitudes of LHCII trimers in A8-35-trapped form, in NA13-trapped form, and in α-DDM solution

Sample	α_1 (%)	τ_1 (ns)	α_2 (%)	τ_2 (ns)	α_3 (%)	τ_3 (ns)	τ_{av} (ns)
A8-35-trapped LHCII	56	3.71	22	1.53	22	0.23	2.46
NA13-trapped LHCII	84	3.84	16	1.23			3.42
LHCII in 0.03 % α-DDM	91	3.84	9	1.31			3.6

Neoxanthin is located at the protein–lipid interface in each monomeric unit of the trimer, partly protruding from the protein (Croce et al. 1999a; Liu et al. 2004) (Fig. 7), which

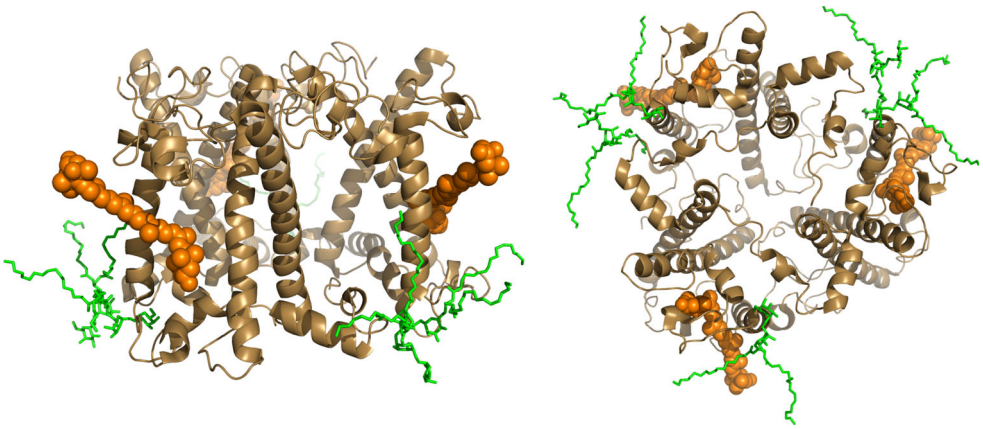

Fig. 7 Crystallographic structure (PDB code 1RWT; Liu et al. 2004) of the LHCII trimer showing neoxanthin (*orange*) and digalactosyl diacylglycerol (*green*) molecules. *Left panel*, view from the mid-plane of the membrane; *right panel*, view normal to the membrane. Other pigments were left out for clarity

makes it a good probe of the local environment of LHCII. It has been used as reporter for the quenched conformation (Ruban et al. 2007). The difference in absorption suggests differences between the A8-35-trapped LHCII and the two other preparations. Similar differences were detected in the CD spectra, in which only one positive peak was observed for the A8-35-trapped LHCII in the region from 470–510 nm, assigned to carotenoids (Croce et al. 1999b), whereas two positive peaks and one negative peak were observed in the same region for LHCII solubilized in α-DDM or trapped by NA13 (Fig. 5). In previous studies, the most pronounced differences between the CD spectra of LHCII from unstacked thylakoid membranes or from lamellar aggregates, on the one hand, and LHCII in β-DDM solution, on the other, have also been seen in the region where carotenoids absorb (Lambrev et al. 2007).

To examine the effect of the two APols on the excited state lifetime of LHCII, time-resolved fluorescence measurements were performed. Fluorescence emission intensity decays are shown in Fig. 6, and the lifetimes and amplitudes collected in Table 1. Whether kept in α-DDM solution or trapped with NA13, LHCII exhibits two lifetime components, one of ~3.8 ns, with amplitudes of 91 and 84 %, respectively, and one of ~1.2–1.3 ns, with amplitudes 9 and 16 % (Table 1). This is in a good agreement with previous measurements carried out with LHCII in β-DDM, the two components being ascribed to the presence of two different LHCII conformations (Moya et al. 2001). A8-35-trapped LHCII differs in exhibiting a short component of 230 ps, representing ~22 % of the total fluorescence. This is indicative of the presence of a sub-population with a new, "quenched" conformation, not observed before for trimeric LHCII in solution (Table 1). As a result, the average lifetime of Chl fluorescence in A8-35-trapped LHCII is ~30 % shorter than in LHCII solubilized in 0.03 % α-DDM or trapped in NA13 (Table 1).

A major chemical difference between α-DDM and NA13, on the one hand, and A8-35, on the other, is that A8-35 carries numerous negative charges, whereas the other two surfactants are non-ionic. To examine the possibility that the electrostatic field created by the carboxylates of A8-35 causes the observed rapid fluorescence decay, time-resolved fluorescence measurements of A8-35-trapped LHCII were performed at various ionic strengths (see "Materials and Methods" section). No changes in lifetime were observed upon increasing the concentration of Na^+ ions from 0 to 500 mM (Table 2). No ionic strength effects were observed either for LHCII in 0.03 % α-DDM, which was used as control (*data not shown*). This seems to exclude a direct effect of the charges of the carboxylates on Chl lifetime. Indeed, MD simulations performed on OmpX/A8-35 complexes (Perlmutter et al. 2014) show that the COO^- groups of A8-35 tend to keep away from the transmembrane surface of the protein, which is, in LHCII, the only region where Chls are exposed to the outside environment of the trimer. It can be concluded that the partial quenching of fluorescence in A8-35-trapped LHCII is due to the different conformation and/or dynamics of the trimer in A8-35 as compared to that in α-DDM and in NA13.

Table 2 Dependence of the fluorescence lifetimes of A8-35-trapped and α-DDM-solubilized LHCII on the ionic strength of the solution

NaCl (mM)	A8-35-trapped LHCII			LHCII in 0.03 % α-DDM	Difference (%)
	τ_{av} (ns)	τ (ns) (shortest component)	α (%) (shortest component)	τ_{av} (ns)	$(\tau_{av\ (DDM)}-\tau_{av(A8\text{-}35)})/\tau_{av\ (DDM)}$
0	2.46	0.23	23	3.6	32
25	2.62	0.29	20	3.6	28
75	2.41	0.12	24	3.6	33
125	2.87	0.21	14	3.6	20
200	2.85	0.38	19	3.6	21
500	2.50	0.3	24	3.6	31

Very strong quenching of the fluorescence of LHCII has been reported in preparations in which the trimer was either in aggregated form or reconstituted in liposomes (Johnson and Ruban 2009; Moya et al. 2001; Pascal et al. 2005). This was ascribed to conformational changes due to protein–protein interactions (Moya et al. 2001). In these measurements, the degree of fluorescence quenching was strongly dependent on the level of aggregation (itself related to the amount of detergent removed from the solution) or on the protein-to-lipid ratio in proteoliposomes. Short components (300–400 ps) were also measured for LHCII incorporated in nanodiscs, but they were proposed to originate from a small number of LHCII aggregates of size <100 nm and to be unrelated to the incorporation of LHCII into nanodiscs (Pandit et al. 2011). Since ultracentrifugation and SEC data exclude the possibility of aggregation of A8-35-trapped LHCII, it can be concluded that the 230-ps component originates from a quenched conformation of trimeric LHCII.

Amphipols Stabilize LHCII Trimers Against Thermal Denaturation

To compare the stability of the trimer in the three environments, CD measurements were carried out as a function of temperature (Fig. 8). Changes of CD values measured at 474 and 680 nm in a temperature range from 20 to 90 °C are shown in Fig. 8d. Apparent T_m values for LHCII in the three environments, obtained from sigmoidal fits of the melting curves at 680 nm (Fig. 8d), are ~65 °C in α-DDM and A8-35 and ~75 °C in NA13. The slopes of the fits indicate more progressive structural changes in NA13 and α-DDM than in A8-35, where the transition is more cooperative. From changes of ellipticity at 474 nm, it can be seen that the unfolding process has a different character in the three environments: the CD signal at 474 nm decreases between ~30 and ~50 °C in α-DDM and between ~50 and ~65 °C in NA13, whereas in A8-35, it stays practically constant till the sharp onset of denaturation at ~60 °C (Fig. 8d, *left panel*). Given that the CD signal at ~470 nm has been assigned to inter-monomer interactions (Georgakopoulou et al. 2007), its decrease in intensity likely results from monomerization. This suggests that, whereas in α-DDM and NA13 the monomerization of LHCII precedes unfolding, this is not the case when LHCII trimer is trapped with A8-35, an interpretation consistent with the greater cooperativity of the denaturation in A8-35. It is worth noting that the monomerization temperature of A8-35-trapped LHCII is comparable to that observed in thylakoid membranes (Dobrikova et al. 2003).

In conclusion, CD data indicate a stabilizing effect of both APols. Thermal denaturation of LHCII in NA13 and α-DDM appears to follow a two-step course, likely to start with monomerization, followed, at higher temperature, by denaturation of the monomers. In NAPol, these two processes are shifted to higher temperatures by ~10 °C with respect to α-DDM. Denaturation in A8-35 starts at about the same temperature as in NA13, but it is more cooperative, probably involving simultaneous monomerization and denaturation. This could reflect the stabilization of the trimer as compared to α-DDM and NA13, and the destabilization of the monomer as compared to NA13. Stabilization of LHCII by APols can presumably be very useful in the study of complexes that are unstable in detergent solution (see Liguori et al. 2013).

Origin of the Differences Between A8-35- and NA13-Trapped LHCII

This is the first time a relatively extended comparison is made between an A8-35-trapped and a NAPol-trapped MP, earlier data being essentially limited to the solution properties of the complexes (Sharma et al. 2012) and the stability of the proteins (Bazzacco et al. 2012). Differences between the denaturation processes in the two polymers have been discussed above. Spectroscopic differences are also quite intriguing. The overall resemblance of all measured features between NAPol-trapped LHCII and LHCII in α-DDM suggests that LHCII in these two environments has probably a similar structure, even though the complex is far more stable in NAPols.

Spectroscopic differences, on the contrary, are noticeable for A8-35-trapped LHCII. The observation that the largest differences between the two APol-trapped preparations seem to be associated with neoxanthin, which protrudes from the transmembrane surface of protein, suggests that this is where the most significant events take place. According to stability and activity measurements (reviewed in Popot et al. 2011) and MD calculations (Perlmutter et al. 2014), A8-35-trapped MPs experience less conformational excursions than their detergent-solubilized counterparts. One possible explanation, therefore, is that A8-35 keeps the LHCII trimer more "tight", which could contribute to its increased stability, and could perhaps also be relevant to the different quenching properties of the Chl. A second possibility is that neoxanthin be more exposed to the aqueous phase in the A8-35-trapped than in the NAPol-trapped or the DDM-solubilized states, due to the difference of thickness of the polar region of the surfactant. Indeed, recent NMR data indicate that tryptophan side chains located at the surface of the major outer MP (MOMP) of *Chlamydia muridarum*—that is in a position akin to that of the outermost extremity of neoxanthin in LHCII—are more exposed to the solution when MOMP is trapped with A8-35 than when it is solubilized by dodecylphosphocholine, a detergent with a moderately large

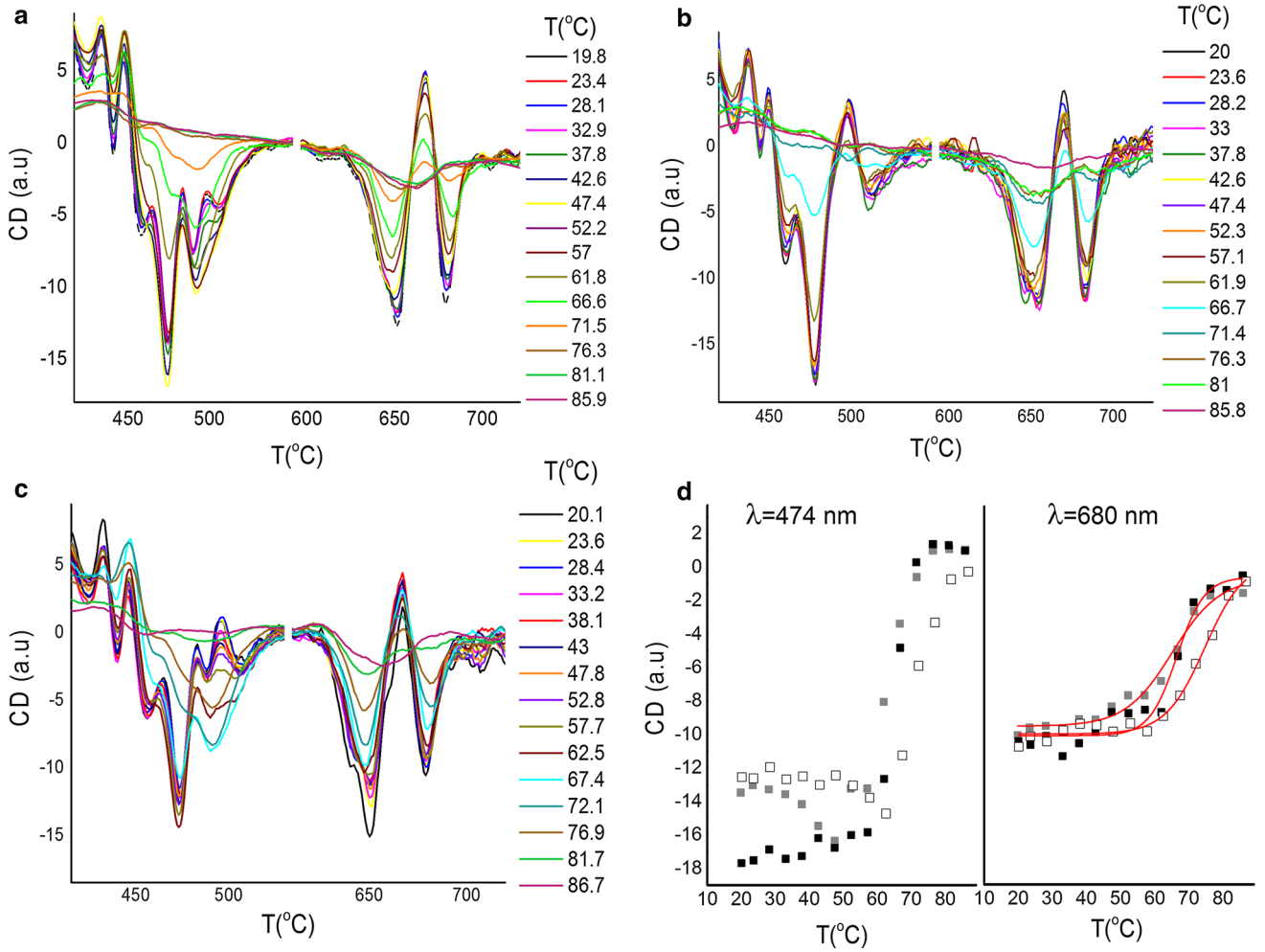

Fig. 8 Circular dichroism of LHCII in 0.03 % α-DDM (**a**), A8-35-trapped LHCII (**b**), and NA13-trapped LHCII (**c**) measured from 20 to 90 °C. Spectra have been smoothed. (**d**) Change of ellipticity at 474 and 680 nm with increasing temperature for LHCII in 0.03 % α-DDM (*grey squares*), trapped with A8-35 (*black squares*) and trapped with NA13 (*black open squares*); sigmoidal fits for the changes at 680 nm are shown in *red*

polar head (Feinstein et al. 2014; Tifrea et al. 2014). Similarly, a polyhistidine tag fused to the *C*–terminus of BR has been observed to be free in A8-35 and buried in DDM (Etzkorn et al. 2014). It may be, therefore, that neoxanthin experiences a more polar environment in A8-35-trapped than in NAPol-trapped LHCII. Finally, a third possible source of differences is related to the competition between surfactants and lipids at the surface of MPs. Functional studies have shown that transferring BR to A8-35 promotes lipid rebinding (Dahmane et al. 2013; for discussions, see Kleinschmidt and Popot 2014; Zoonens and Popot 2014). Lipid rebinding to LHCII could obviously influence the spectroscopic properties of the surface-exposed neoxanthin. On would have to assume, however, that the interaction of NAPol-trapped LHCII with lipids resembles that in DDM more than that in A8-35. Whereas such a proposal is clearly very speculative, it may perhaps be that the relatively long C_{11} alkyl chains of NAPols have more affinity for lipid-binding sites at the surface of LHCII, and that they compete more efficiently for binding to them, than the short C_8 chains of A8-35.

Conclusions

In conclusion, we present evidence that the two APols tested have stabilizing effects on LHC complexes, A8-35 exhibiting a significant stabilizing effect on the trimeric LHCII, whereas NA13 stabilizes the monomers. APols thus appear as potentially useful tools to study other LHC complexes, some of which are unstable in detergent solution. It is interesting also to note that in A8-35, part of the Chl exhibits a very short lifetime, in the total absence of protein aggregation. Taken together, the present observations open new

avenues for studying native and recombinant antenna proteins at neutral and basic pH using A8-35, and in a broader range of pH using NAPols.

Acknowledgments Particular thanks are due to Roberta Croce (VU University Amsterdam) for her support and help throughout this work, as well as for contributing to its writing. We also thank Laura M. Roy and Bart Sasbrink (VU University Amsterdam) for critical reading of the manuscript, and Pengqi Xu for his help with generating Fig. 7. This project was supported by the Chemical Science division of the Netherlands organization for scientific research (NWO-CW) via an ECHO grant to R. Croce, by the CNRS, by University Paris-7, and by the "Initiative d'Excellence" program from the French State (Grant "DYNAMO", ANR-11-LABX-0011-01).

References

Althoff T, Mills DJ, Popot J-L, Kühlbrandt W (2011) Assembly of electron transport chain components in bovine mitochondrial supercomplex $I_1III_2IV_1$. EMBO J 30:4652–4664

Ballottari M, Girardon J, Dall'Osto L, Bassi R (2012) Evolution and functional properties of Photosystem II light harvesting complexes in eukaryotes. Biochim Biophys Acta 1817:143–157

Barros T, Royant A, Standfuss J, Dreuw A, Kühlbrandt W (2009) Crystal structure of plant light-harvesting complex shows the active, energy-transmitting state. EMBO J 28:298–306

Bassi R, Simpson D (1987) Chlorophyll-protein complexes of barley photosystem-I. Eur J Biochem 163:221–230

Bazzacco P, Billon-Denis E, Sharma KS, Catoire LJ, Mary S, Le Bon C, Point E, Banères J-L, Durand G, Zito F, Pucci B, Popot J-L (2012) Non-ionic homopolymeric amphipols: application to membrane protein folding, cell-free synthesis, and solution NMR. Biochemistry 51:1416–1430

Belgio E, Johnson MP, Jurić S, Ruban AV (2012) Higher plant photosystem II light-harvesting antenna, not the reaction center, determines the excited-state lifetime-both the maximum and the nonphotochemically quenched. Biophys J 102:2761–2771

Bowie JU (2001) Stabilizing membrane proteins. Curr Opin Struct Biol 11:397–402

Breyton C, Tribet C, Olive J, Dubacq J-P, Popot J-L (1997) Dimer to monomer conversion of the cytochrome b_6f complex: causes and consequences. J Biol Chem 272:21892–21900

Caffarri S, Croce R, Cattivelli L, Bassi R (2004) A look within LHCII: differential analysis of the Lhcbl-3 complexes building the major trimeric antenna complex of higher-plant photosynthesis. Biochemistry 43:9467–9476

Caffarri S, Passarini F, Bassi R, Croce R (2007) A specific binding site for neoxanthin in the monomeric antenna proteins CP26 and CP29 of Photosystem II. FEBS Lett 581:4704–4710

Croce R, Zucchelli G, Garlaschi FM, Bassi R, Jennings RC (1996) Excited state equilibration in the photosystem I light-harvesting I complex: P700 is almost isoenergetic with its antenna. Biochemistry 35:8572–8579

Croce R, Remelli R, Varotto C, Breton J, Bassi R (1999a) The neoxanthin binding site of the major light harvesting complex (LHCII) from higher plants. FEBS Lett 456:1–6

Croce R, Weiss S, Bassi R (1999b) Carotenoid-binding sites of the major light-harvesting complex II of higher plants. J Biol Chem 274:29613–29623

Croce R, Canino G, Ros F, Bassi R (2002) Chromophore organization in the higher-plant photosystem II antenna protein CP26. Biochemistry 41:7334–7343

Croce R, van Amerongen H (2011) Light-harvesting and structural organization of photosystem II: from individual complexes to thylakoid membrane. J Photochem Photobiol, B 104:142–153

Dahmane T, Giusti F, Catoire LJ, Popot J-L (2011) Sulfonated amphipols: synthesis, properties and applications. Biopolymers 95:811–823

Dahmane T, Rappaport F, Popot J-L (2013) Amphipol-assisted folding of bacteriorhodopsin in the presence or absence of lipids: functional consequences. Eur Biophys J 42:85–101

Diab C, Tribet C, Gohon Y, Popot J-L, Winnik FM (2007) Complexation of integral membrane proteins by phosphorylcholine-based amphipols. Biochim Biophys Acta 1768:2737–2747

Dobrikova AG, Várkonyi Z, Krumova SB, Kovács L, Kostov GK, Todinova SJ, Busheva MC, Taneva SG, Garab G (2003) Structural rearrangements in chloroplast thylakoid membranes revealed by differential scanning calorimetry and circular dichroism spectroscopy. Thermo-optic effect. Biochemistry 42:11272–11280

Etzkorn M, Zoonens M, Catoire LJ, Popot J-L, Hiller S (2014) How amphipols embed membrane proteins: global solvent accessibility and interaction with a flexible protein terminus. J Membr Biol. doi:10.1007/s00232-014-9657-9

Feinstein HE, Tifrea D, Sun G, Popot J-L, de la Maza LM, Cocco MJ (2014) Long-term stability of a vaccine formulated with the amphipol-trapped major outer membrane protein from *Chlamydia trachomatis*. J Membr Biol. doi:10.1007/s00232-014-9693-5

Garavito RM, Ferguson-Miller S (2001) Detergents as tools in membrane biochemistry. J Biol Chem 276:32403–32406

Georgakopoulou S, van der Zwan G, Bassi R, van Grondelle R, van Amerongen H, Croce R (2007) Understanding the changes in the circular dichroism of light harvesting complex II upon varying its pigment composition and organization. Biochemistry 46:4745–4754

Gilmore AM, Yamamoto HY (1991) Zeaxanthin formation and energy-dependent fluorescence quenching in pea chloroplasts under artificially mediated linear and cyclic electron transport. Plant Physiol 96:635–643

Giusti F, Popot J-L, Tribet C (2012) Well-defined critical association concentration and rapid adsorption at the air/water interface of a short amphiphilic polymer, amphipol A8-35: a study by Förster resonance energy transfer and dynamic surface tension measurements. Langmuir 28:10372–10380

Giusti F, Rieger J, Catoire L, Qian S, Calabrese AN, Watkinson TG, Casiraghi M, Radford SE, Ashcroft AE, Popot J-L (2014) Synthesis, characterization and applications of a perdeuterated amphipol. J Membr Biol. doi:10.1007/s00232-014-9656-x

Gohon Y, Giusti F, Prata C, Charvolin D, Timmins P, Ebel C, Tribet C, Popot J-L (2006) Well-defined nanoparticles formed by hydrophobic assembly of a short and polydisperse random terpolymer, amphipol A8-35. Langmuir 22:1281–1290

Gohon Y, Dahmane T, Ruigrok R, Schuck P, Charvolin D, Rappaport F, Timmins P, Engelman DM, Tribet C, Popot J-L, Ebel C (2008) Bacteriorhodopsin/amphipol complexes: structural and functional properties. Biophys J 94:3523–3537

Jansson S (1999) A guide to the Lhc genes and their relatives in *Arabidopsis*. Trends Plant Sci 4:236–240

Johnson MP, Ruban AV (2009) Photoprotective energy dissipation in higher plants involves alteration of the excited state energy of the emitting chlorophyll(s) in the light harvesting antenna II (LHCII). J Biol Chem 284:23592–23601

Kleinschmidt JH, Popot J-L (2014) Folding and stability of integral membrane proteins in amphipols (submitted).

Lambrev PH, Várkonyi Z, Krumova S, Kovács L, Miloslavina Y, Holzwarth AR, Garab G (2007) Importance of trimer–trimer interactions for the native state of the plant light-harvesting complex II. Biochim Biophys Acta 1767:847–853

Levi V, Rossi JP, Echarte MM, Castello PR, Gonzalez Flecha FL (2000) Thermal stability of the plasma membrane calcium pump. Quantitative analysis of its dependence on lipid-protein interactions. J Membr Biol 173:215–225

Liao M, Cao E, Julius D, Cheng Y (2014) Single particle electron cryo-microscopy of a mammalian ion channel. Curr Opin Struct Biol 27:1–7

Liguori N, Roy LM, Opačić M, Durand G, Croce R (2013) Regulation of light-harvesting in the green alga *Chlamydomonas reinhardtii*: the *C*-terminus of LHCSR is the knob of a dimmer switch. J Am Chem Soc 135:18339–18342

Liu ZF, Yan HC, Wang KB, Kuang TY, Zhang JP, Gui LL, An XM, Chang WR (2004) Crystal structure of spinach major light-harvesting complex at 2.72 Å resolution. Nature 428:287–292

Lund S, Orlowski S, de Foresta B, Champeil P, le Maire M, Møller JV (1989) Detergent structure and associated lipid as determinants in the stabilization of solubilized Ca^{2+}-ATPase from sarcoplasmic reticulum. J Biol Chem 264:4907–4915

Miloslavina Y, Wehner A, Lambrev PH, Wientjes E, Reus M, Garab G, Croce R, Holzwarth AR (2008) Far-red fluorescence: a direct spectroscopic marker for LHCII oligomer formation in non-photochemical quenching. FEBS Lett 582:3625–3631

Morosinotto T, Mozzo M, Bassi R, Croce R (2005) Pigment-pigment interactions in Lhca4 antenna complex of higher plants photosystem I. J Biol Chem 280:20612–20619

Moya I, Silvestri M, Vallon O, Cinque G, Bassi R (2001) Time-resolved fluorescence analysis of the photosystem II antenna proteins in detergent micelles and liposomes. Biochemistry 40:12552–12561

Mozzo M, Morosinotto T, Bassi R, Croce R (2006) Probing the structure of Lhca3 by mutation analysis. Biochim Biophys Acta 1757:1607–1613

Müller P, Li XP, Niyogi KK (2001) Non-photochemical quenching. A response to excess light energy. Plant Physiol 125:1558–1566

Nagy JK, Kuhn Hoffmann A, Keyes MH, Gray DN, Oxenoid K, Sanders CR (2001) Use of amphipathic polymers to deliver a membrane protein to lipid bilayers. FEBS Lett 501:115–120

Natali A, Roy LM, Croce R (2014) In vitro reconstitution of light-harvesting complexes of plants and green algae. J Vis Exp. doi:10.3791/51852

Pandit A, Shirzad-Wasei N, Wlodarczyk LM, van Roon H, Boekema EJ, Dekker JP, de Grip WJ (2011) Assembly of the major light-harvesting complex II in lipid nanodiscs. Biophys J 101:2507–2515

Pascal AA, Liu ZF, Broess K, van Oort B, van Amerongen H, Wang C, Horton P, Robert B, Chang WR, Ruban A (2005) Molecular basis of photoprotection and control of photosynthetic light-harvesting. Nature 436:134–137

Perlmutter JD, Popot J-L, Sachs JN (2014) Molecular dynamics simulations of a membrane protein/amphipol complex. J Membr Biol. doi:10.1007/s00232-014-9690-8

Picard M, Dahmane T, Garrigos M, Gauron C, Giusti F, le Maire M, Popot J-L, Champeil P (2006) Protective and inhibitory effects of various types of amphipols on the Ca2+-ATPase from sarcoplasmic reticulum: a comparative study. Biochemistry 45:1861–1869

Polovinkin V, Gushchin I, Balandin T, Chervakov P, Round E, Schevchenko V, Popov A, Borshchevskiy V, Popot J-L, Gordeliy V (2014) High-resolution structure of a membrane protein transferred from amphipol to a lipidic mesophase. J Membr Biol doi:10.1007/s00232-014-9700-x

Popot J-L (2010) Amphipols, nanodiscs, and fluorinated surfactants: three non-conventional approaches to studying membrane proteins in aqueous solutions. Annu Rev Biochem 79:737–775

Popot J-L, Althoff T, Bagnard D, Banères J-L, Bazzacco P, Billon-Denis E, Catoire LJ, Champeil P, Charvolin D, Cocco MJ, Crémel G, Dahmane T, de la Maza LM, Ebel C, Gabel F, Giusti F, Gohon Y, Goormaghtigh E, Guittet E, Kleinschmidt JH, Kühlbrandt W, Le Bon C, Martinez KL, Picard M, Pucci B, Rappaport F, Sachs JN, Tribet C, van Heijenoort C, Wien F, Zito F, Zoonens M (2011) Amphipols from A to Z. Annu Rev Biophys 40:379–408

Privé GG (2007) Detergents for the stabilization and crystallization of membrane proteins. Methods 41:388–397

Rosenbusch JP (2001) Stability of membrane proteins: relevance for the selection of appropriate methods for high-resolution structure determinations. J Struct Biol 136:144–157

Ruban AV, Berera R, Ilioaia C, van Stokkum IHM, Kennis JTM, Pascal AA, van Amerongen H, Robert B, Horton P, van Grondelle R (2007) Identification of a mechanism of photoprotective energy dissipation in higher plants. Nature 450:575–578

Ruban AV, Johnson MP, Duffy CDP (2012) The photoprotective molecular switch in the photosystem II antenna. Biochim Biophys Acta 1817:167–181

Sharma KS, Durand G, Pucci B (2011) Synthesis and determination of polymerization rate constants of glucose-based monomers. Des Monomers Polym 14:499–513

Sharma KS, Durand G, Gabel F, Bazzacco P, Le Bon C, Billon-Denis E, Catoire LJ, Popot J-L, Ebel C, Pucci B (2012) Non-ionic amphiphilic homopolymers: synthesis, solution properties, and biochemical validation. Langmuir 28:4625–4639

Tifrea D, Pal S, Cocco MJ, Popot J-L, de la Maza LM (2014) Increased immuno accessibility of MOMP epitopes in a vaccine formulated with amphipols may account for the very robust protection elicited against a vaginal challenge with *C. muridarum*. J Immunol 192:5201–5213

Tribet C, Audebert R, Popot J-L (1996) Amphipols: polymers that keep membrane proteins soluble in aqueous solutions. Proc Natl Acad Sci USA 93:15047–15050

Tribet C, Audebert R, Popot J-L (1997) Stabilization of hydrophobic colloidal dispersions in water with amphiphilic polymers: application to integral membrane proteins. Langmuir 13: 5570–5576

Tribet C, Diab C, Dahmane T, Zoonens M, Popot J-L, Winnik FM (2009) Thermodynamic characterization of the exchange of detergents and amphipols at the surfaces of integral membrane proteins. Langmuir 25:12623–12634

van Oort B, van Hoek A, Ruban AV, van Amerongen H (2007) Aggregation of light-harvesting complex II leads to formation of efficient excitation energy traps in monomeric and trimeric complexes. FEBS Lett 581:3528–3532

van Oort B, Amunts A, Borst JW, van Hoek A, Nelson N, van Amerongen H, Croce R (2008) Picosecond fluorescence of intact and dissolved PSI-LHCI crystals. Biophys J 95:5851–5861

Wientjes E, Oostergetel GT, Jansson S, Boekema EJ, Croce R (2009) The role of Lhca complexes in the supramolecular organization of higher plant photosystem I. J Biol Chem 284:7803–7810

Wientjes E, van Amerongen H, Croce R (2013) LHCII is an antenna of both photosystems after long-term acclimation. Biochim Biophys Acta 1827:420–426

Zoonens M, Giusti F, Zito F, Popot J-L (2007) Dynamics of membrane protein/amphipol association studied by Förster resonance energy transfer. Implications for in vitro studies of amphipol-stabilized membrane proteins. Biochemistry 46:10392–10404

Zoonens M, Popot J-L (2014) Amphipols for each season. J Membr Biol. doi:10.1007/s00232-014-9666-8